Supporting information

Comb-like ionic complexes of poly(γ-glutamic acid) and alkanoylcholines derived from fatty acids

A. Tolentino,[†] S. León, [‡] A. Alla,[†] A. Martínez de Ilarduya,[†] and S. Muñoz-Guerra[†]*

†Departament d'Enginyeria Química, Universitat Politècnica de Catalunya, ETSEIB, Diagonal 647, Barcelona 08028, Spain

‡Departamento de Ingeniería Química, Universidad Politécnica de Madrid, ETSIIM, Gutiérrez Abascal 2, Madrid 28006, Spain

Content: Table of thermal properties of *n*ACh·I. Compared ^{1}H-NMR spectra of *n*ACh·PGGA. SAXS and WAXS profiles at variable temperature of *n*ACh·PGGA. TEM micrographs of 14ACh·PGGA and 16ACh·PGGA cryosectioned films. Table of conformational angles of PGGA helices. Radial distribution function of methylene units in the paraffinic phase. This material is available free of charge via the Internet at http://pubs.acs.org.

Table 1. Synthesis data of alkoylcholine iodides.

*n*ACh·I	Yield (%)	T_m[a] (ºC)	T_d[b] (ºC)
12ACh·I	Powder (white)	83/169	197
14ACh·I	Powder (white)	93/164	207
16ACh·I	Crystalline powder (white)	99/163	209
18ACh·I	Crystalline powder (white)	104/161	209

[a] T_m, Melting temperature obtained from DSC from pristine samples.
[b] T_d, Onset decomposition temperature determined from TGA traces by the tangent method.

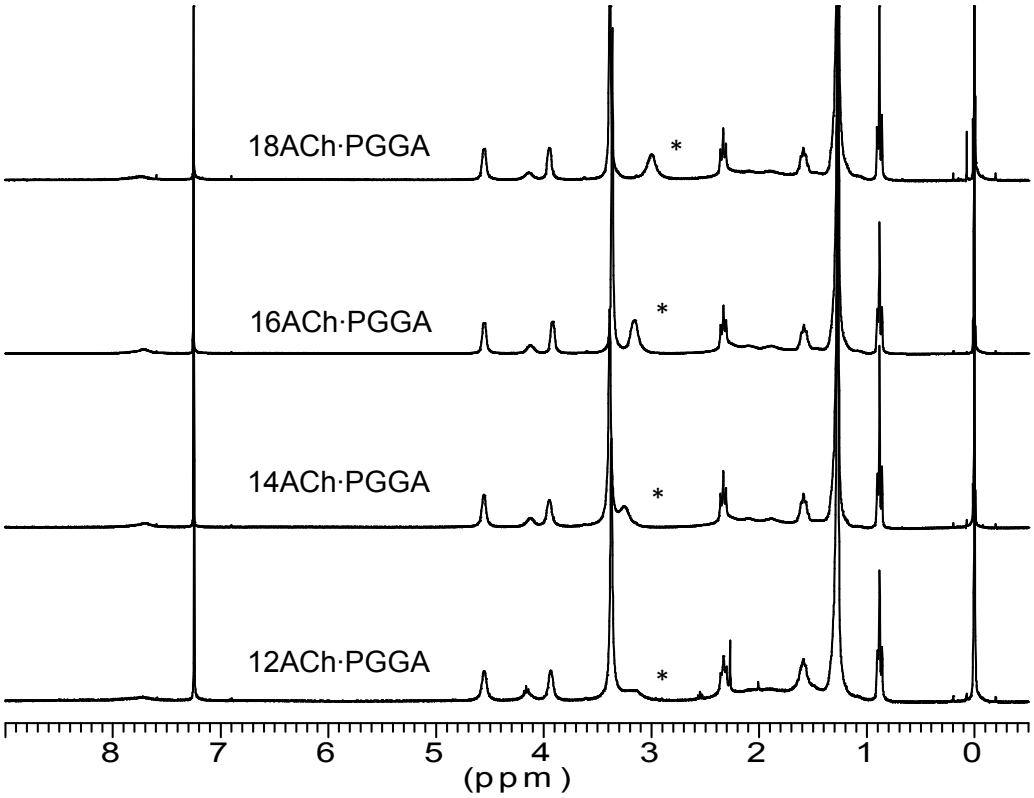

Figure 1. Compared ^{1}H NMR spectra of *n*ACh·PGGA in $CDCl_3$. (*) Peak of residual water.

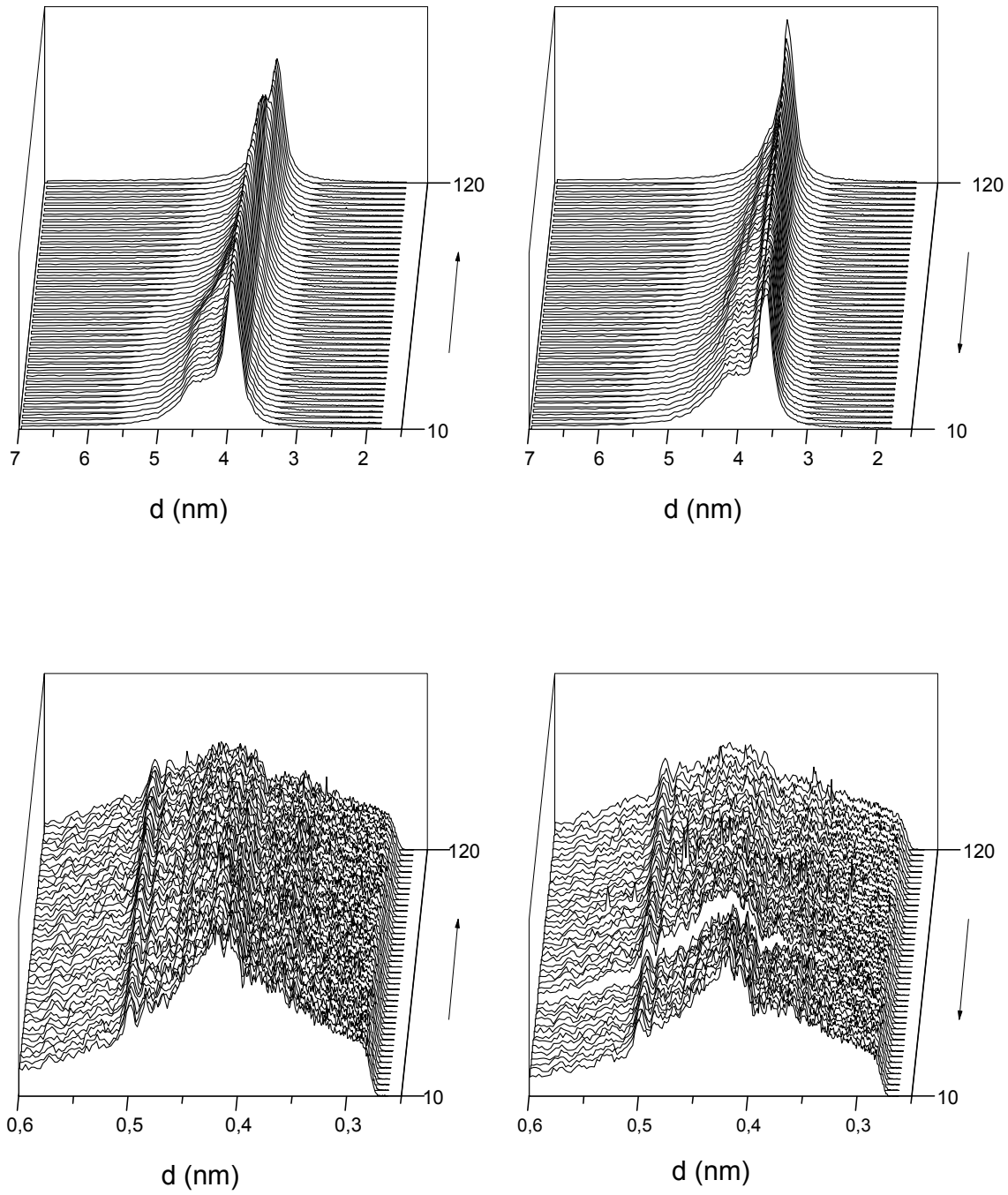

Figure 2. SAXS (top) and WAXS (bottom) profiles of 12ACh·PGGA at heating and cooling.

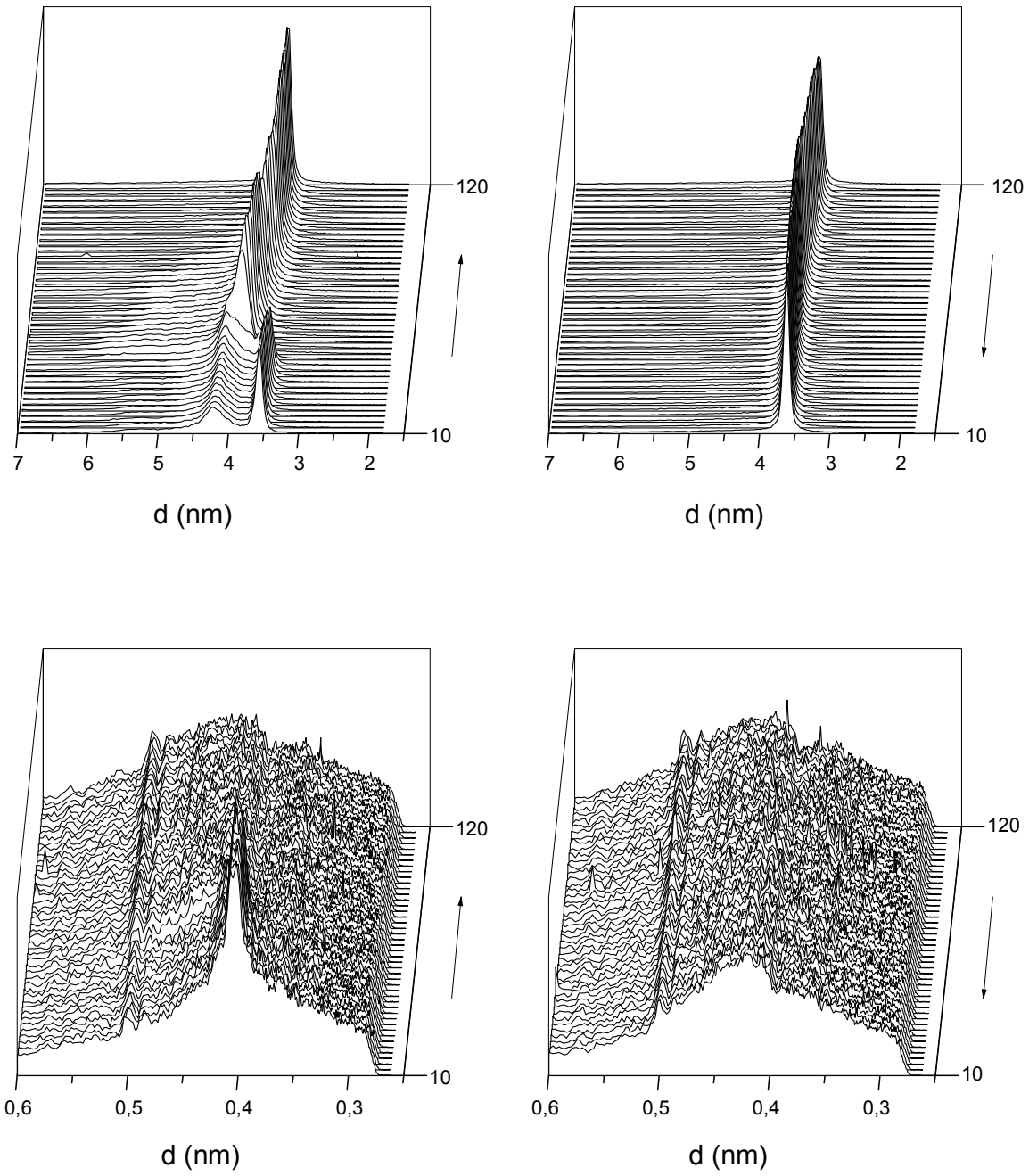

Figure 3. SAXS (top) and WAXS (bottom) profiles of 14ACh·PGGA at heating and cooling.

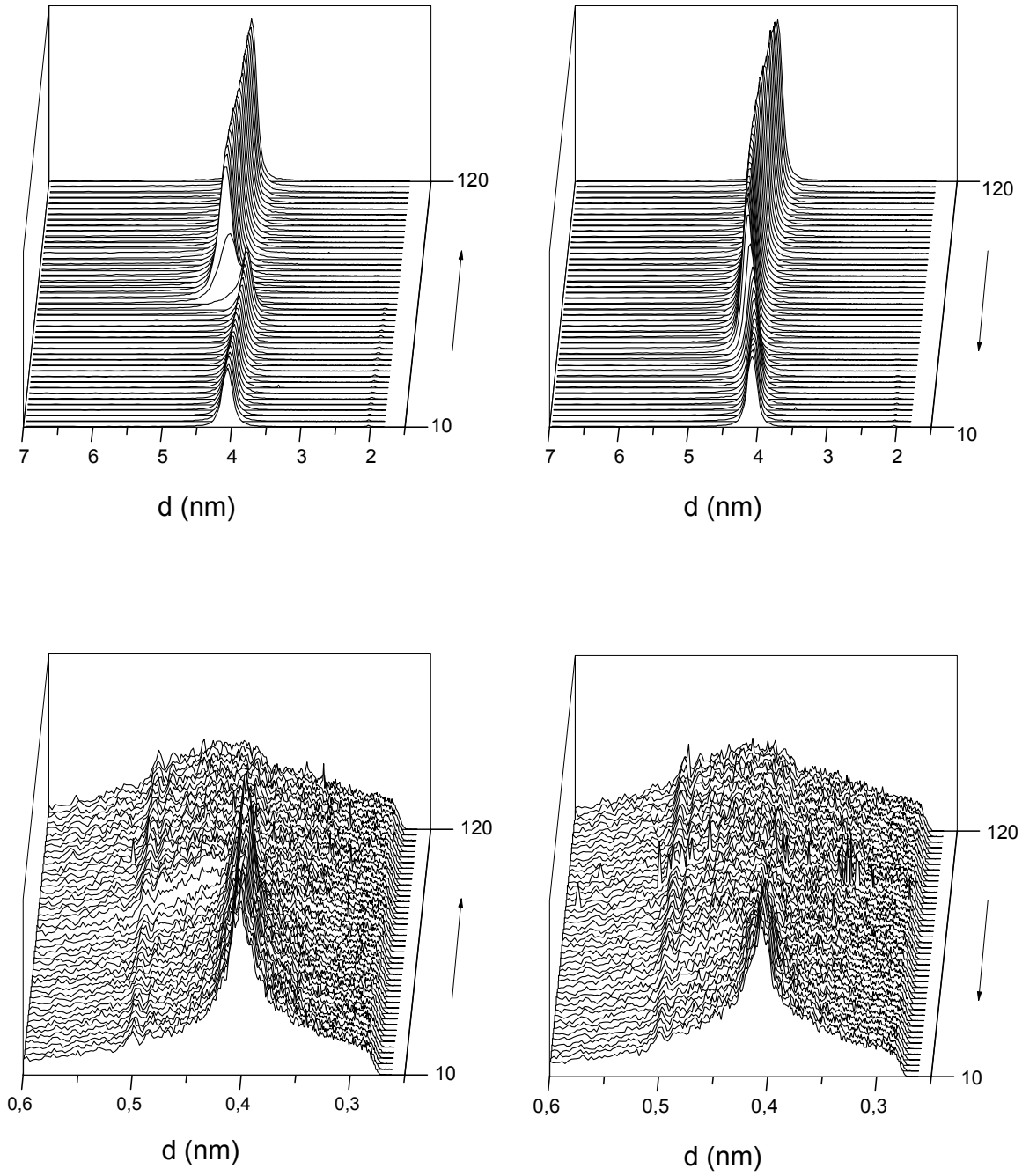

Figure 4. SAXS (top) and WAXS (bottom) profiles of 18ACh·PGGA at heating and cooling.

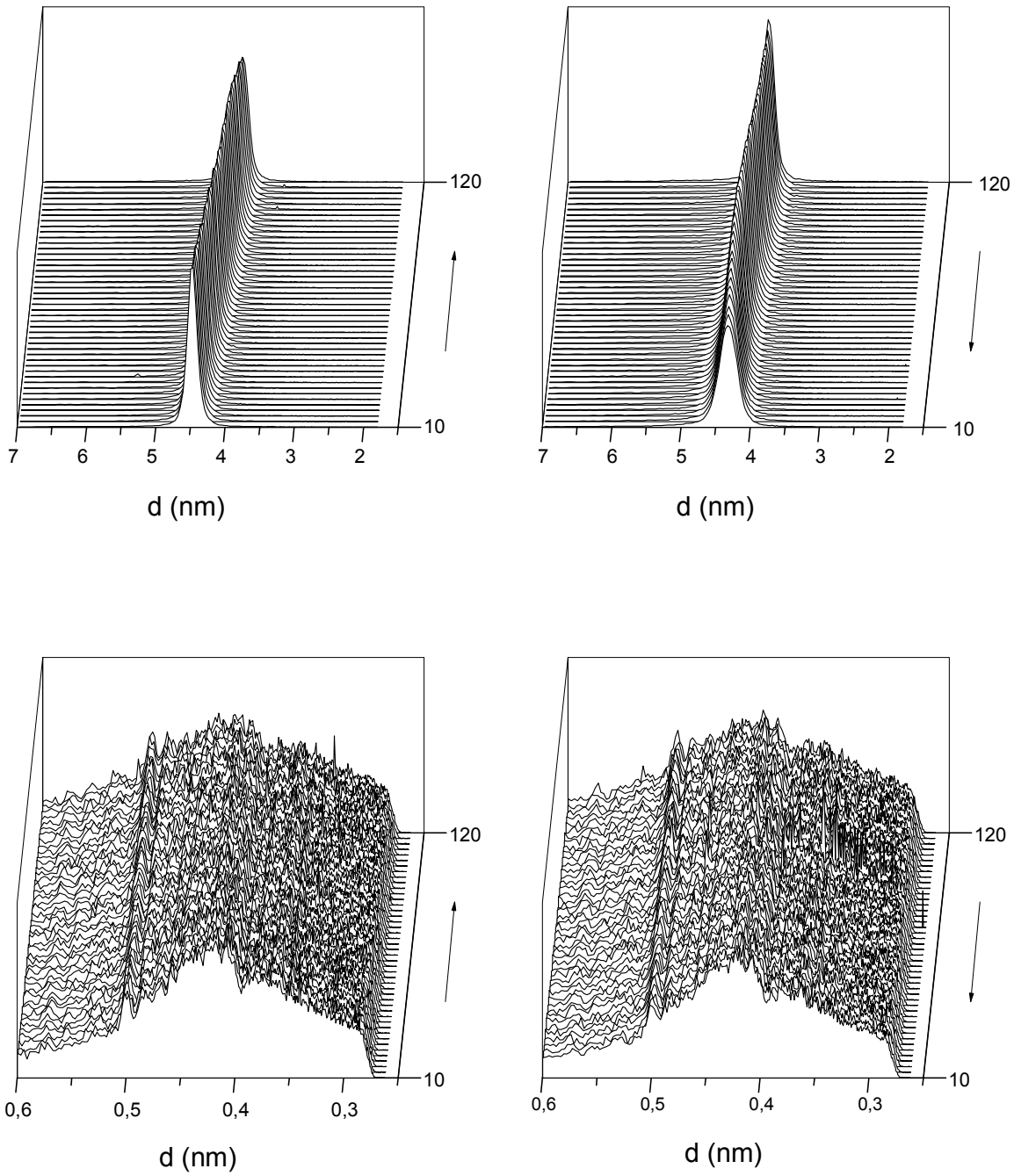

Figure 5. SAXS (top) and WAXS (bottom) profiles of 18*c*ACh·PGGA at heating and cooling.

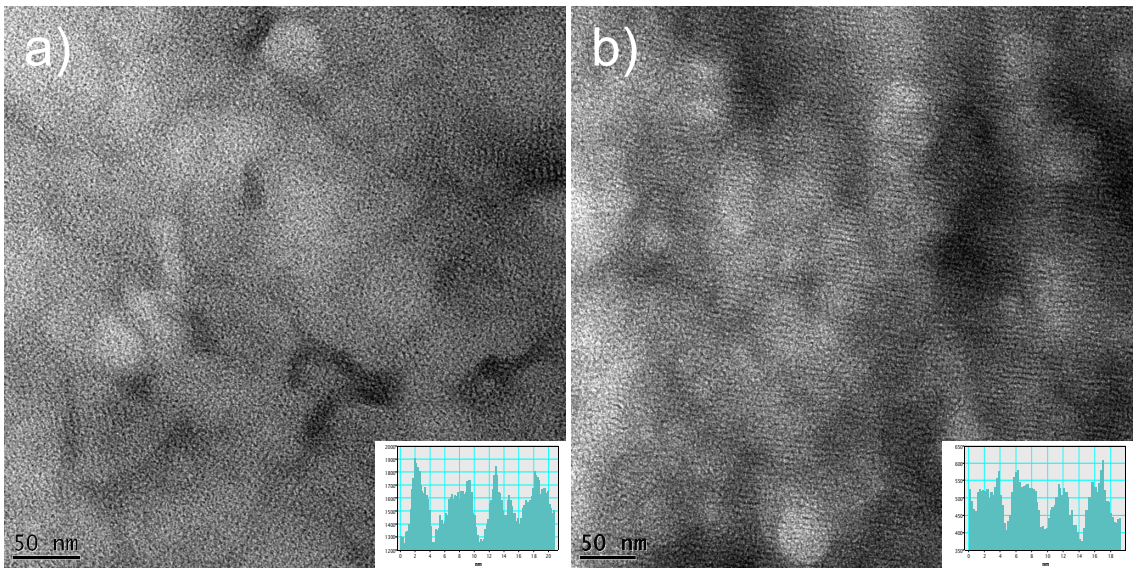

Figure 6. TEM images of 14ACh·PGGA a) and 16ACh·PGGA b) films obtained by casting. Insets: Optical density profiles showing the structural periodicity observed in each case.

Table 2. Conformational angles and parameters for the helical conformations considered in this work. Comparison of starting values with those obtained after geometry optimization.				
	5/2		**17/5**	
	Starting	**Optimized**	**Starting**	**Optimized**
φ	-137.9	-132.7	70.9	58.0
ξ_1	53.0	60.6	52.8	56.4
ξ_2	75.6	64.8	-171.0	-173.6
ψ	-143.8	-147.0	159.9	167.8
Rise per residue	2.02	2.02	1.50	1.48

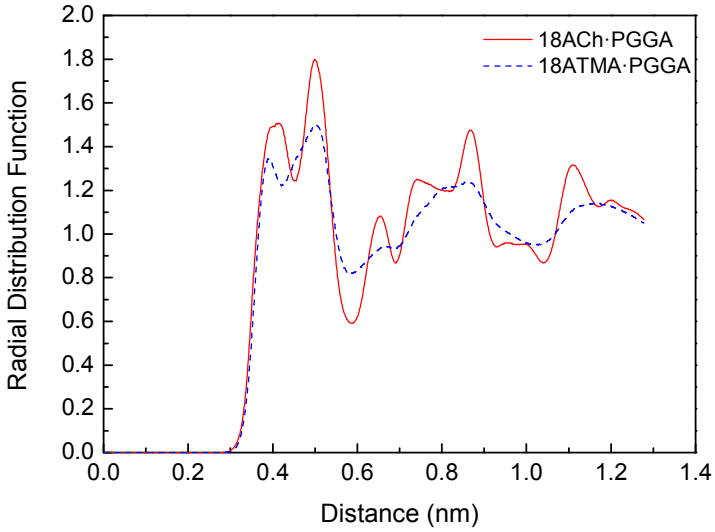

Figure 7. Comparison of the intermolecular radial distribution function for the methylene and methyl groups of the side-chains as a function of the distance for 18ACh·PGGA (red solid line) and 18ATMA·PGGA (blue dashed line) complexes from molecular dynamics simulations at room temperature (298 K).